Draft version February 5, 2008
Preprint typeset using LaTeX style emulateapj v. 6/22/04

ON THE VIABILITY OF BIANCHI TYPE VII$_H$ MODELS WITH DARK ENERGY

T. R. Jaffe[1], S. Hervik[2], A. J. Banday[1], K. M. Górski[3]

(Dated:)
Draft version February 5, 2008

ABSTRACT

We generalize the predictions for the CMB anisotropy patterns arising in Bianchi type VII$_h$ universes to include a dark energy component. We consider these models in light of the result of Jaffe et al. (2005a,b) in which a correlation was found on large angular scales between the *WMAP* data and the anisotropy structure in a low density Bianchi universe. We find that by including a term $\Omega_\Lambda > 0$, the same best-fit anisotropy pattern is reproduced by several combinations of cosmological parameters. This sub-set of models can then be further constrained by current observations that limit the values of various cosmological parameters. In particular, we consider the so-called geometric degeneracy in these parameters imposed by the peak structure of the *WMAP* data itself. Apparently, despite the additional freedom allowed by the dark energy component, the modified Bianchi models are ruled out at high significance.

Subject headings: cosmology: cosmic microwave background – cosmology: observations

1. INTRODUCTION

While cosmology appears to be converging on a "concordance model" that describes the universe as inflationary and isotropic, there remain unexplained anomalies in the CMB data, and other models are not yet ruled out. The *WMAP* data provide some of the most accurate measurements yet of the cosmic microwave background and contribute to high accuracy determinations of cosmological parameters (Bennett et al. 2003; Spergel et al. 2003). However, there are several studies that show that at large scales, the CMB is not statistically isotropic and Gaussian, as predicted by inflation theory (de Oliveira-Costa et al. 2004; Eriksen et al. 2004; Hansen et al. 2004b; Vielva et al. 2004).

In Jaffe et al. (2005a,b), we examined a particular set of anisotropic cosmological models: the Bianchi type VII$_h$ class of spatially homogeneous generalizations of Friedmann universes that include small vorticity (universal rotation) and shear (differential expansion) components. Surprisingly, we found evidence that one of these models correlates with the CMB sky and that subtracting this component resolves several of these observed anomalies. The models used in that study were derived by Barrow et al. (1985) and include no cosmological constant component in the total energy density. The best-fit model found by that study required $\Omega_{\rm m0} = 0.5$, implying, $\Omega_k = 0.5$, i.e., a significantly negatively curved universe.

Land & Magueijo (2005) subsequently considered flat Bianchi models and sought explicitly to resolve the problems of the low quadrupole and the low-ℓ alignments using a statistic constructed to achieve that purpose. Their analysis does indeed find a model that fixes these anomalies, but it remains statistically insignificant as a detection. Our original result has the benefit of being a detection that is based entirely on a simple least-squares fit of the Bianchi template to the data, yet we find that it serendipitously resolves several anomalies without that requirement having been built-in to the search algorithm. The importance of our result, therefore, lies in the fact that it resolves the problems of the low quadrupole, low-ℓ alignments, power asymmetry, and non-Gaussian cold spot.

However, both analyses neglect the fact that the existing Bianchi solutions include no dark energy component. Furthermore, the best-fit results require an energy content that is consistent neither with other astronomical observations nor with the CMB itself. In this work, we present a modification of the Barrow et al. Bianchi type VII$_h$ solution so that it includes a cosmological constant term in the evolution. We discuss the impact of that term on the structure of the resulting CMB anisotropy pattern, particularly the degeneracy that is introduced in the model space by the addition of Ω_Λ. We then discuss the viability of Λ models that are morphologically identical to our best-fit $\Omega_\Lambda = 0$ models by considering the constraints imposed by different measurements of the cosmological parameters.

2. BIANCHI MODELS WITH $\Lambda > 0$

2.1. *Solution*

First we shall generalize the equations in Barrow et al. (1985) to include a cosmological constant Λ. The basic assumption is that the type VII$_h$ universe is close to FRW.

We start with the equations of motion using expansion-normalized variables (see, e.g., Wainwright & Ellis 1997). The equations describing the evolution of Bianchi type VII$_h$ universes with a tilting perfect fluid can be found in Coley & Hervik (2005) and Hervik et al. (2005a). In our case, we consider a tilting perfect fluid with $\gamma = 1$ (dust) and a cosmological constant. The equations in Coley & Hervik (2005) can easily be generalized to include a cosmological constant by adding a matter term $(\Omega_\Lambda, \gamma_\Lambda = 0)$ wherever there is a matter

[1] Max-Planck-Institut für Astrophysik, Karl-Schwarzschild-Str. 1, Postfach 1317, D-85741 Garching bei München, Germany; tjaffe@MPA-Garching.MPG.DE, banday@MPA-Garching.MPG.DE.
[2] Dept. of Mathematics and Statistics, Dalhousie University, Halifax, Nova Scotia, B3H 3J5, Canada; herviks@mathstat.dal.ca
[3] JPL, M/S 169/327, 4800 Oak Grove Drive, Pasadena CA 91109; Warsaw University Observatory, Aleje Ujazdowskie 4, 00-478 Warszawa, Poland; Krzysztof.M.Gorski@jpl.nasa.gov

term (Ω, γ).

Furthermore, we assume that the universe is close to a FRW at all times and that the tilt velocity of the dust fluid is small; hence we assume:

$$\Sigma^2 \ll 1,\ |\mathbf{N}_\times| \ll 1,\ v_1 \ll 1,\ |\mathbf{v}| \ll 1. \tag{1}$$

Here, $\Sigma^2 = \sigma^2/(3H^2)$ is the expansion-normalized shear scalar, $\mathbf{N}_\times$ is a complex curvature variable, and v_1, $\mathbf{v} = v_2 + iv_3$ are the tilt components (see Coley & Hervik 2005 for details). The curvature variables A and $\bar{N}$ need not be small, and they are related to the group parameter h as follows:

$$A^2 \approx 3h\bar{N}^2.$$

We also assume that the parameter h is not too small: $h \geq \mathcal{O}(1)$. (As $h \to 0$, the assumptions made for this derivation break down and a qualitatively different solution for type VII_0 is needed. See Hervik et al. 2005b.)

Given the above assumptions, the deceleration parameter is

$$q \approx \frac{1}{2}\Omega_\mathrm{m} - \Omega_\Lambda, \tag{2}$$

and the equation of motion for the Hubble scalar is

$$H' = -(q+1)H, \tag{3}$$

where the prime indicates the derivative with respect to the dimensionless time T defined by $dt/dT = 1/H$, and t is the cosmological time.

At the lowest order, the tilt components that are related to the vorticity are the components $v_2 + iv_3 \equiv \mathbf{v}$ (in the notation of Coley & Hervik 2005). These induce non-zero shear components $\Sigma_{12} + i\Sigma_{13} \equiv \mathbf{\Sigma}_1$ via the linear constraint equation, which in the FRW limit reduces to:

$$\mathbf{\Sigma}_1\bar{N}(i - 3\sqrt{h}) + \Omega_\mathrm{m}\mathbf{v} = 0. \tag{4}$$

Moreover, close to FRW the curvature $K \equiv A^2$ and matter densities Ω_m and Ω_Λ are related via the Friedmann equation

$$1 = \Omega_\Lambda + K + \Omega_\mathrm{m}. \tag{5}$$

We also define x to be

$$x \equiv \left(\frac{h}{K_0}\right)^{\frac{1}{2}} = \left(\frac{h}{1 - \Omega_{\Lambda 0} - \Omega_{\mathrm{m}0}}\right)^{\frac{1}{2}}. \tag{6}$$

Eq. (4) now reduces to Barrow et al.'s eqs.(4.6) and (4.7) by dropping the subscript 0 and replacing Ω with Ω_m. The equations of motion can now be solved.

By choosing $T_0 = 0$, $x = e^{\alpha_0}H_0$, we can relate z to T and the time variable τ in Barrow et al. (1985) to the redshift z:

$$1 + z = e^{-T}, \tag{7}$$

$$\frac{dT}{d\tau} = He^T e^{\alpha_0}. \tag{8}$$

The Hubble scalar, K, Ω_m, and Ω_Λ can then be written

$$H(z) = H_0\mathcal{H}(z), \tag{9}$$

$$\mathcal{H}(z) = \left[\Omega_{\Lambda 0} + K_0(1+z)^2 + \Omega_{\mathrm{m}0}(1+z)^3\right]^{\frac{1}{2}}, \tag{10}$$

$$K = \frac{K_0(1+z)^2}{\mathcal{H}^2(z)}, \tag{11}$$

$$\Omega_\mathrm{m} = \frac{\Omega_{\mathrm{m}0}(1+z)^3}{\mathcal{H}^2(z)}, \tag{12}$$

$$\Omega_\Lambda = \frac{\Omega_{\Lambda 0}}{\mathcal{H}^2(z)}, \tag{13}$$

where $\Omega_{\Lambda 0}, K_0, \Omega_{\mathrm{m}0}$ are the present values of the expansion-normalized Λ, curvature and ordinary matter (dust) and obey the constraint:

$$1 = \Omega_{\Lambda 0} + K_0 + \Omega_{\mathrm{m}0}.$$

We also note that $K = \Omega_k > 0$ implies negative curvature. The shear components Σ_{12} and Σ_{13}, and the remaining curvature variable are given by

$$\Sigma_{12} = \frac{\Sigma_{12,0}(1+z)^3}{\mathcal{H}(z)}, \tag{14}$$

$$\Sigma_{13} = \frac{\Sigma_{13,0}(1+z)^3}{\mathcal{H}(z)}, \tag{15}$$

$$\bar{N} = \frac{\bar{N}_0(1+z)}{\mathcal{H}(z)}. \tag{16}$$

Conformal time becomes

$$\tau - \tau_0 = -\frac{1}{x}\int_0^z \frac{dz}{\mathcal{H}(z)}, \tag{17}$$

which can be used in the Barrow expressions for s and ψ. The integrals of Barrow et al. equations (4.12) and (4.13) become

$$\int_0^{z_E} \frac{s(1-s^2)\sin\psi(1+z)^2 dz}{(1+s^2)^2\mathcal{H}(z)} \tag{18}$$

$$\int_0^{z_E} \frac{s(1-s^2)\cos\psi(1+z)^2 dz}{(1+s^2)^2\mathcal{H}(z)} \tag{19}$$

with $C_3 = 4$, where z_E is the redshift at photon emission. In calculating the constant C_1, the density Ω_0 should now be $\Omega_{\mathrm{m}0}$, i.e. the matter density only.

The following assumptions should be kept in mind regarding this solution:

- The tilt velocity is small. In a dust- or Λ-dominated Bianchi type VII_h universe, the tilt asymptotically tends to zero at late times. Using the above relations, it can also be shown that for the case of interest, it remains small back to the last scattering surface as well.

- The universe is close to FRW at all times. This assumption is required to make the problem tractable. In a Λ-dominated universe, the type VII_h models become close to FRW. For the cases in question, plugging the numbers into the above relations shows that this assumption still holds at the surface of last scattering. (At very early times, however, this is not the case.) It is likely that models for which this assumption does not hold at last scattering would then have greater shear effects, but the details would require a more complicated derivation.

- Barrow et al. (1985) only consider the contribution from the vorticity that directly involves the shear variables Σ_{12} and Σ_{13}. The (expansion-normalized) shear scalar, $\Sigma^2 = \sigma^2/(3H^2)$, is given by

$$\Sigma^2 = \Sigma_+^2 + |\mathbf{\Sigma}_\times|^2 + \Sigma_{12}^2 + \Sigma_{13}^2 \qquad (20)$$

and involves therefore all of the shear components. In Barrow et al. (1985) and here, the other shear components have simply been ignored in the calculation of $\Delta T/T$. Considering additional shear degrees of freedom is in principle possible but in practice difficult. The effect of such additions is one of the largest unknowns in this analysis.

2.2. *Properties*

In the presence of the cosmological constant, a universe that is very nearly flat now and that was very nearly flat at the time of last scattering can become significantly negatively curved at intermediate redshifts. We can see this from Eqtn. 11 above.

Figure 1 shows how $K(z)$ evolves for different values of $\Omega_{\Lambda 0}$ and $\Omega_{\rm m0}$. At high redshift, the matter dominates and the curvature vanishes, and at low redshift, Ω_Λ can dominate, depending on its exact value. At intermediate redshifts, however, the universe may become more negatively curved. For a currently almost flat universe with parameters close to the observed values of $\Omega_{\Lambda 0} \sim 0.7$ and $\Omega_{\rm m0} \sim 0.3$, the curvature is at most only a few percent (black curve). Only for very small matter densities and very large dark energy densities does the curvature become large at intermediate redshifts. To reproduce the observed asymmetry with these $\Lambda > 0$ models requires either a large current negative curvature (pink and blue dot-dashed curves) or a very small matter density (green dashed curve).

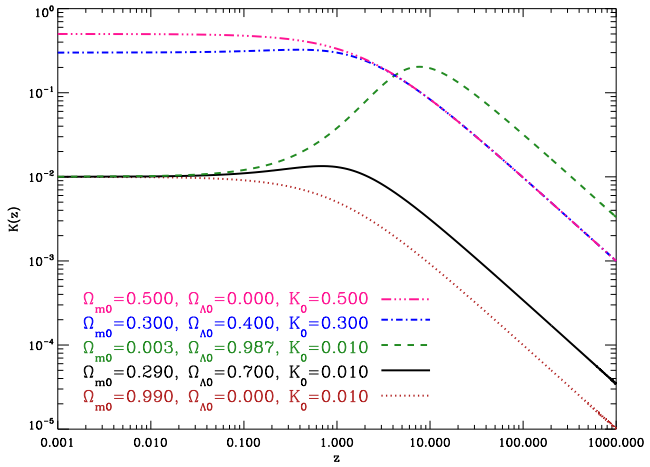

FIG. 1.— Examples of the evolution of $K(z)$. See text.

The addition of a Λ component adds a third parameter to the Bianchi parameter space, but there is a degeneracy to the resulting morphology of the Bianchi-induced pattern. The same structure in the induced anisotropy pattern can be reproduced by different parameter combinations. The addition of dark energy results in a tighter spiral for a given value of x, because the redshift to the surface of last scattering corresponds to a larger time difference. The geodesics have therefore completed more rotations since recombination for a given value of x when $\Omega_\Lambda > 0$. Secondly, the focusing of the spiral depends on the curvature between the observer and the last scattering surface. Significant focusing can arise from a universe that is very open now, or from a universe where Λ is large enough to give negative curvature at intermediate redshifts (as shown in Fig. 1.)

Three combinations of parameters, for example, can reproduce the same apparent structure on the sky :

1. $(x, \Omega_{\Lambda 0}, \Omega_{\rm m0}) = (0.62, 0, 0.5)$ – i.e., no Λ and a matter content half critical, giving a large current negative curvature (the model found in Jaffe et al. 2005b);

2. $(x, \Omega_{\Lambda 0}, \Omega_{\rm m0}) = (0.8, 0.4, 0.3)$ – i.e., approximately the observed matter content (baryon plus dark) , with some Λ but still a large current negative curvature;

3. $(x, \Omega_{\Lambda 0}, \Omega_{\rm m0}) = (4.0, 0.987, 0.003)$ – i.e., a much smaller than observed matter content, but a nearly flat current curvature ($\Omega_k = 0.01$); the large Λ causes a large negative curvature at intermediate redshifts.

The real difference between these models is the amplitude: (3) has an amplitude $\sim 80\%$ of (1), and (2) has an amplitude of ~ 8 *times* that of (1). The shear and vorticity values obtained from fitting these templates to the data would change accordingly.

Effectively, this implies that a given structure on the sky characterized by the amount of geodesic focusing and the number of spiral turns is the same for all models along a line in the three dimensional parameter space of $(\Omega_{\rm k0}, \Omega_{\Lambda 0}, x)$. The degeneracy in the templates is only broken by the amplitude of the variation. But $(\sigma/H)_0$ is what we measure by fitting a template to the sky, so we cannot distinguish among the degenerate models without an independent measurement of the shear.

It is not straightforward to calculate where such lines of degeneracy lie. Instead, we determine this empirically by generating a grid of models and comparing them to the previously determined best-fit model.

3. VIABILITY OF A BIANCHI TYPE VII$_H$ MODEL

We now address the question of whether the degeneracy of the Bianchi type VIIh models with $\Omega_{\Lambda 0} > 0$ described in §2 gives us enough freedom to define a Bianchi model that is morphologically identical to the best-fit model in Jaffe et al. (2005a,b) and that is also consistent with estimates of the cosmological parameters.

3.1. *Matter Density and 'Geometric' Degeneracy*

Efstathiou & Bond (1999) describe the limitations of constraining cosmological parameters with CMB data alone. In particular, there is a 'geometric' degeneracy in the curvature and dark energy density (or equivalently, the matter density.) Degenerate models have: 1) the same values of the physical baryon density , $\omega_{\rm b} = \Omega_{\rm b} h^2$, and cold dark matter density, $\omega_{\rm c} = \Omega_{\rm c} h^2$; 2) the same

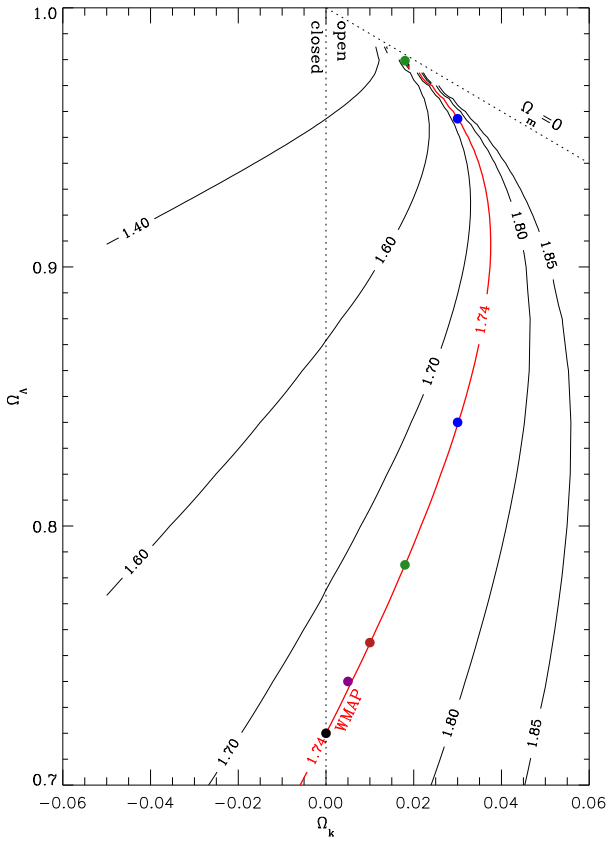

FIG. 2.— Degeneracy contours on the $\Omega_\Lambda - \Omega_k$ plane for $\omega_b = 0.023$ and $\omega_m = 0.13$. Along the red line denoting $\mathcal{R}$ for the *WMAP* best-fit parameters, the circles mark example power spectra that are shown in Figure 3.

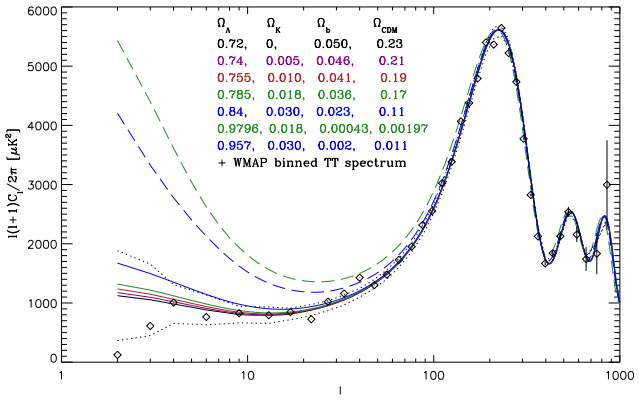

FIG. 3.— Power spectra for several models degenerate with the *WMAP* data (marked with circles in figure 2.) The solid versus dashed green and blue curves are where there are two degenerate models at the same value of Ω_k; the dashed is that with the higher Ω_Λ. The spectra are normalized so that the amplitude at the first acoustic peak is always the same. The dotted black line shows the cosmic variance uncertainty for each data point around the *WMAP* model.

primordial fluctuation spectrum; and 3) the same value of the parameter

$$\mathcal{R} = \sqrt{\frac{\omega_m}{\omega_k}} \begin{cases} \sinh[\sqrt{\omega_k} y] & \text{if } \omega_k > 0, \\ \sqrt{\omega_k} y & \text{if } \omega_k = 0, \\ \sin[\sqrt{\omega_k} y] & \text{if } \omega_k < 0, \end{cases} \tag{21}$$

where

$$y = \int_{a_{rec}}^{1} \frac{da}{\sqrt{\omega_m a + \omega_k a^2 + \omega_\Lambda a^4}} \tag{22}$$

(where a_{rec} is the scale factor at recombination). These models will have almost the same power spectra. Contours of constant $\mathcal{R}$ in model space Ω_k versus Ω_Λ are shown in Figure 2, with red highlighting the curve intersecting the best-fit, flat, *WMAP*-only parameters (Spergel et al. 2003, Table 1). Figure 3 shows power spectra for those degenerate models (calculated using CMBFAST.[4]) When normalized, the spectra are identical at the acoustic peaks, and the degeneracy only fails at large angular scales.

In the three dimensional parameter space of $(\Omega_{k0}, \Omega_{\Lambda 0}, x)$, the geometric degeneracy forms a surface, while the Bianchi models with identical structure form a line. The two need not intersect, but in the case of the observed *WMAP* CMB-only power spectrum of Spergel et al. (2003) and best-fit Bianchi model of Jaffe et al. (2005a,b), they do. There is a Bianchi model that has the identical structure to the best-fit $\Omega_\Lambda = 0$ model and lies on the *WMAP* degeneracy curve. It has parameters $(\Omega_{k0}, \Omega_{\Lambda 0}, x) = (0.028, 0.96, 2.5)$. But how viable is this region of parameter space?

As shown in Figure 3, the geometric degeneracy is broken at large angular scales. Models with high $\Omega_{\Lambda 0}$ and low Ω_{m0} predict too much large scale power. *WMAP* data alone place relatively loose constraints on Ω_{m0}, but even these rule out such low values as required for the Bianchi models. (The power spectrum of the sky corrected for the Bianchi component has less large-scale power overall (Jaffe et al. 2005a,b) than the uncorrected power shown in that figure, so the problem will only become worse.)

To quantify these limits, we examine the posterior likelihood from the *WMAP* data alone using the COSMOMC[5] code of Lewis & Bridle (2003), which implements a Monte Carlo Markov Chain method. For a simple look to compare the *WMAP* constraints to the Bianchi degeneracy, we explore the five-parameter space of: θ (the ratio of the sound horizon to the angular diameter distance), τ (optical depth), Ω_k (curvature), n_s (spectral index of scalar perturbations), and A_s (amplitude of scalar perturbations), with fixed parameters $\omega_b = 0.023$ (the physical baryon density), $\omega_{dm} = 0.107$ (the physical dark matter density), $f_\nu = 0$ (neutrino fraction of dark matter density), $w = -1$ (dark energy equation of state), $r \equiv A_t/A_s = 0$ (ratio of tensor to scalar fluctuations). Other parameters such as H_0, $\Omega_{\Lambda 0}$, and Ω_{m0} are derived from this set. (The free parameters have only such priors as defined by ranges that are much broader than any realistic uncertainty.) The resulting constraints in the $\Omega_m - \Omega_\Lambda$ plane (marginalizing over the other parameters) are shown in Figure 4 in red. All Bianchi models with the structure of the best-fit model lie well outside the 95% confidence region from the *WMAP* data alone.

[4] http://www.cmbfast.org/

[5] http://cosmologist.info/cosmomc/

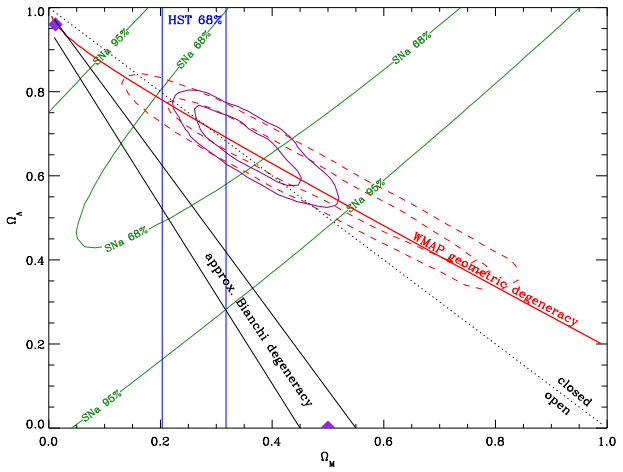

FIG. 4.— Parameter space by $\Omega_{\rm m}$. In green are the supernovae constraints (Knop et al. 2003). The solid red line is the same geometric degeneracy curve shown in Figure 2. In blue are the HST Key Project (Freedman et al. 2001) constraints from $\Omega_{\rm m0} = \omega_{\rm m}/h^2$ (assuming fixed $\omega_{\rm m}$ and $\omega_{\rm c}$). The black solid lines show an approximate representation of where the Bianchi degeneracy lies, from the original model at $(x, \Omega_{\Lambda 0}, \Omega_{\rm m0}) = (0.62, 0, 0.5)$ to the one that lies on the *WMAP* geometric degeneracy curve at $(0.028, 0.96, 2.5)$ (each shown with a violet diamond.) The likelihood contours from *WMAP* data alone (computed using cosmomc; see text) are shown with the red dashed lines. In solid magenta are the contours from *WMAP*, supernovae, HST, and SDSS data combined, where $\omega_{\rm m}$ and $\omega_{\rm c}$ also vary.

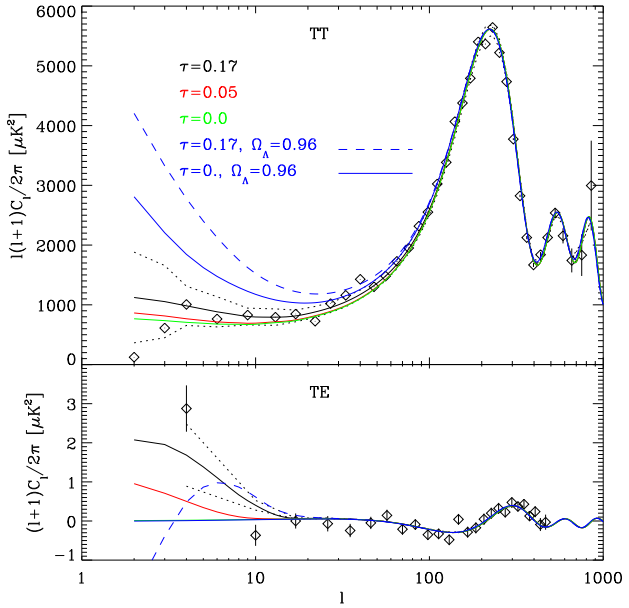

FIG. 5.— Power spectra as a function of optical depth, τ, each normalized such that the first peak heights are all the same (effectively changing A_s.) The top panel is the TT power, and the bottom the TE cross-power. Lowering τ lowers the large scale power, but not enough to bring the high Ω_Λ models down to the range of the data.

Allowing the physical matter densities to vary as well but including other datasets, the constraints (in magenta) are even tighter.

Tegmark et al. (2004) give $\Omega_{\rm m0} = 0.57^{+0.45}_{-0.33}$ from *WMAP* data alone, which tightens to $\Omega_{\rm m0} = 0.40^{+0.10}_{-0.09}$ adding data from the Sloan Digital Sky Survey (SDSS). See also Sanchez et al. (2005) for CMB+2dFGRS results.

3.2. *Optical Depth*

Figure 3 shows that the geometric degeneracy breaks at large angular scales, and the models with high Ω_Λ have too much large scale power. But there is an additional degeneracy if we allow the optical depth, τ, to vary. Adjusting τ and $A_{\rm s}$ such that $A_{\rm p} \equiv A_{\rm s} e^{-2\tau}$ remains constant has exactly the effect we need of modifying only the large scale power while leaving the peak heights unchanged (Tegmark et al. 2004). Figure 5 shows how this works, but that the effect is not large enough. Even a τ of zero does not bring the power at large angular scales within range of the data, and that model is inconsistent with the large-scale peak in the TE spectrum.

One can also ask if the addition of the Bianchi component can affect the variance of the large scale TE cross-power, resulting in an incorrect estimate of τ due to a chance alignment of the polarization signal with the Bianchi structure. Simulations with no reionization and with an added Bianchi temperature pattern (the same location and shear amplitude as our best-fit model) show that this is not the case. The cross-power remains flat at low ℓ with the expected variance.

Note that Hansen et al. (2004a) find different values of τ derived from fitting temperature data in the Northern and Southern hemispheres as defined in the frame of reference that maximizes the power asymmetry (see Hansen et al. 2004b.) The additional large-scale structure in the South that the Bianchi template reproduces could cause this effect. If a polarization signal were also produced in a Bianchi geometry and correlated with the temperature anisotropy, it would influence the measured optical depth from the low-ℓ TE peak as well.

3.3. *Supernovae, H_0, etc.*

The degeneracy contours in Figure 2 are plotted for constant values of $\omega_{\rm m} = 0.13$ and $\omega_{\rm b} = 0.023$ (from Spergel et al. 2003). For different points in the $(\Omega_{k0}, \Omega_{\Lambda 0})$ space, $\Omega_{\rm m0}$ changes and therefore the value of $h \equiv H_0/(100\ {\rm km\ s^{-1} Mpc^{-1}})$ changes, increasing with increasing $\Omega_{\Lambda 0}$ along the degeneracy curve. For models of high $\Omega_{\Lambda 0}$ that lie on the geometric degeneracy curve, H_0 reaches values over 300. This is ruled out at high significance by the *WMAP* data itself; Tegmark et al. (2004) give $H_0 = 48^{+27}_{-12} {\rm km\ s^{-1} Mpc^{-1}}$. Independent determinations of Hubble's constant also rule out these values, e.g., the HST Key Project (Freedman et al. 2001) value of $72 \pm 8 {\rm km\ s^{-1} Mpc^{-1}}$. See, e.g., Spergel et al. (2003, Table 3) for other estimates of the Hubble constant.

High-redshift supernovae observations can break the geometric degeneracy by independently placing constraints that are nearly perpendicular to the *WMAP* constraints in $\Omega_{\rm m} - \Omega_\Lambda$ space (see Figure 4.) The degeneracy curve for the best-fit Bianchi model compared to the *WMAP* data lies outside the 98% confidence contour determined by the Supernova Cosmology Project (Knop et al. 2003, fit no. 6).

It is worth pointing out that it is not clear whether

type Ia supernovae are truly standard candles out to high redshift. The uncertainty, however, is not enough to accommodate such low values of $\Omega_{\rm m0}$.

The addition of cosmic vorticity and shear would, of course, influence the determinations of such parameters. The sky coverage of supernova, for example, is fairly extensive outside the Galactic Plane region, but the sample size is small. Studies such as Kolatt & Lahav (2001) have ruled out significant dipole or quadrupole asymmetry in the expansion, but a test for a more complicated anisotropy structure induced by the vorticity would require far more supernova in the sample and a good sky coverage. Furthermore, as the current value of the shear expansion is very small, distance measurements to relatively low red-shift (compared to the CMB) objects may not be sensitive enough to detect it. This also implies that such a small current shear would not significantly alter measurements of other cosmological parameters such as the Hubble constant that are dependent on relatively low-redshift observations.

3.4. *Other Bianchi Models*

One can also ask, then, how much one can vary the parameters of the Bianchi model and still have a statistically significant fit. The most interesting region on Figure 4 is near $(\Omega_{\rm m}, \Omega_\Lambda) = (0.15, 0.75)$, where the *WMAP* and supernovae constraints approach the region of the best-fit Bianchi model. This model resembles the best-fit model, but since it is closer to flat than the Bianchi degeneracy curve, there is less geodesic focusing. As a result, the model is not so good a fit to the data, and has a significance, compared to Gaussian realizations, of only 85%, compared to over 99% for the model at the same Ω_Λ but on the Bianchi degeneracy curve.

Considering that the *WMAP* data somewhat favor a closed universe, one might ask about closed models with vorticity and shear. These are Bianchi type IX models, also discussed in Barrow et al. (1985). Unlike the open type VII$_h$ models, however, closed models exhibit neither geodesic focusing nor the spiral pattern, even in the presence of vorticity. Barrow et al. use them to place limits on vorticity and shear simply using the quadrupole. Such closed models do not reproduce the morphology needed to explain the power asymmetry or the cold spot, and it would be impossible to claim any detection with only the quadrupole as an observable.

3.5. *Other Dark Energy Models*

The cosmological constant is the simplest form of dark energy, and all observations so far remain consistent with it. Other models are not ruled out, however, and in some cases are favored. Alternatives come in many varieties, some with physical motivation, others constructed to give a particular result. (See, e.g., Padmanabhan 2003.) Here, we address the question of whether an alternative dark energy model can bring our Bianchi pattern any closer to the constraints imposed by the data.

Dark energy models are characterized by their equation of state, $p = w\rho$, where a cosmological constant Λ corresponds to a model with a constant $w = -1$. Alternative theories allow w to vary with time, as in "quintessence" and "k-essence" models. A rather *ad hoc* parameterization is often used of the form $w = w_0 + w_1 z$, which allows comparison of generic dark energy models with supernova data (Wang et al. 2004; Dicus & Repko 2004).

The derivation in §2 can be generalized for any dark energy model by the appropriate substitution into equations 10 and 13 of Ω_X instead of Ω_Λ. We then have

$$\mathcal{H}(z)^2 = \Omega_{X0} f_X(z) + K_0(1+z)^2 + \Omega_{\rm m0}(1+z)^3 \quad (23)$$

where the function f_X is derived from the equation of state as

$$f_X = \exp\left\{3\int_0^z \frac{dz'}{1+z'}\,(1+w(z'))\right\} \quad (24)$$

Examples for extreme values of w_0 and w_1 are shown in Figure 6. As was shown in Figure 1, we can look at the evolution of the curvature as a function of time for these models and see if any display the required negative curvature at intermediate redshift. Using this parameterization, or alternatively the parameterization $w = w_0 + w_1 \frac{z}{z+1}$, does not give much additional freedom, however, to create a viable model. Ultimately, the amount of curvature and therefore focusing is still largely a function of the relative densities of matter and dark energy and of the current curvature. Manipulating the evolution of the dark energy equation of state simply changes the time scales on which the transitions between the different components of the density occur.

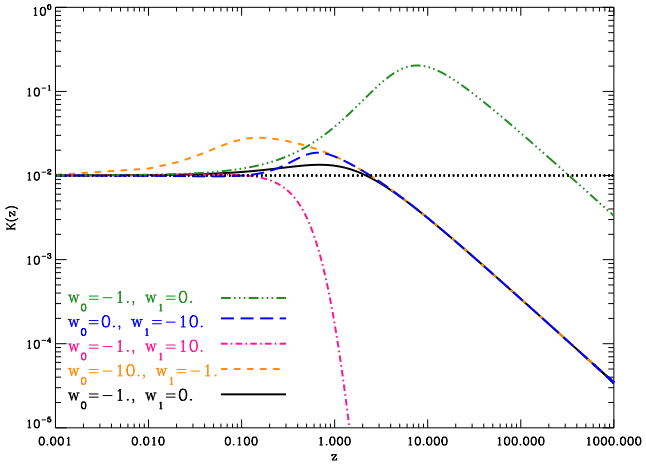

FIG. 6.— Examples of the evolution of $K(z)$ for different dark energy models where the current curvature is constrained to be small ($K_0 = 0.01$). $\Omega_{\rm m0} = 0.29$ for all except the green triple-dot-dashed curve, where $\Omega_{\rm m0} = 0.003$. This is the curve shown in Fig. 1 with a small matter density, high Ω_Λ, and approximately the amount of curvature needed to create the best-fit Bianchi model.

3.6. *Small-scale Structure*

We have so far ignored an additional issue with these models related to the stochastic component of the CMB. The analysis in Jaffe et al. (2005a,b) assumes that the observed CMB anisotropies consist of two independent signals: the predicted Bianchi pattern, and a stochastic, statistically isotropic component. The latter may be generated via inflation or another mechanism, but if it is statistically isotropic at the surface of last scattering, it might no longer be statistically isotropic when observed after traveling through a Bianchi universe.

The power spectrum at small scales might deviate from predictions due to additional structure (dependent on

orientation relative to the preferred axis) introduced by propagation in a Bianchi metric. We note that the asymmetry observed in Eriksen et al. (2004) and Hansen et al. (2004b) extends to $\ell \sim 40$, while the Bianchi model has structure only up to $\ell \sim 15$. Geodesic focusing might cause such a power asymmetry, though it might also require that the asymmetry continue to the smallest angular scales, which is not observed. Hansen et al. (2004b) also find that some unexplained outliers in the *WMAP* power spectrum are associated with different hemispheres.

Furthermore, the generation of the fluctuations at the last scattering surface might also be affected by the anisotropy, though in the case in question, that anisotropy remains very small ($\lesssim 10^{-4}$) at $z \sim 1000$. Essentially, we expect that the Bianchi models could also be constrained by the lack of deviations in the power spectrum from the best-fit *WMAP*/concordance model, although detailed predictions for such deviations are needed.

The consistency of the acoustic peak scale with the flat concordance model would be very difficult for our best-fit Bianchi model to explain.

3.7. *Early Universe*

Considering the success of Big Bang Nucleosynthesis in explaining light element abundances, any model that significantly changes the physical processes at those early times must be ruled out. Several studies have thus attempted to place limits on shear expansion and rotation by examining their effect on the relative Helium abundance, Y. Barrow (1976) originally showed that such analysis can place strong constraints on shear. The interesting exception, however, was type VII$_h$ models, where Barrow found that the CMB remained a stronger constraint. Later studies showed that including more complicated effects can reverse the trend of Y with the shear (see, e.g., Juszkiewicz et al. 1983). Barrow (1984) revisited the issue and showed that in some cases, even extremely anisotropic models may still have the observed Helium abundance. Bianchi type VII$_h$ models, however, have not been treated in detail since the result of Barrow (1976). After demonstrating for several cases, not including VII$_h$, that Y increases for anisotropic models, Matzner et al. (1986) *conjecture* that the same trend applies for *all* anisotropic models, but they admit that this is difficult to prove.

In short, it is possible that such Bianchi models are strongly ruled out by BBN and the observed Helium fraction. But this has not been definitively proved.

4. DISCUSSION AND CONCLUSIONS

We have presented solutions for Bianchi type VII$_h$ type universes that include a dark energy term and examined how their morphological properties change over the parameter space. The addition of dark energy adds a degeneracy such that different combinations of the three parameters $(\Omega_{\rm m}, \Omega_\Lambda, x)$ can lead to the same observed structure as in the best-fit model of Jaffe et al. (2005a,b). A template can be constructed that has the identical structure of that best-fit model and also falls on the geometric degeneracy curve for the parameters as measured by *WMAP* data.

This model, however, lies well outside the 95% confidence region in $\Omega_{\rm m}-\Omega_\Lambda$ space for *WMAP* data, ruled out by the over-prediction of large scale power. It also lies outside the 95% likelihood contours from the Supernova Cosmology Project, and is further inconsistent with the measurement of the Hubble constant from the Hubble Key Project. Bianchi models that are more consistent with these other measurements are no longer good fits to the *WMAP* large scale structure.

One of the most difficult problems for these models is to account for the acoustic peak structure. The anisotropy at early times might influence the nature of the fluctuations at last scattering, and the geometry could affect the power spectrum on small angular scales due to the geodesic focusing between last scattering and the observer. Detailed predictions for these effects would be needed, but it is difficult to envision such an anisotropic scenario that happened to reproduce the observed acoustic peak structure, mimicking the concordance cosmology so well.

There is currently no prediction for the CMB polarization anisotropy in a Bianchi universe, but such a geometry-induced signal could provide an additional test of these models. If the preferred direction indicated in the temperature data is also reflected in the full sky polarization data (expected from further *WMAP* data releases and, eventually, from Planck), there will be even more motivation to consider non-standard models.

We have shown that our best-fit Bianchi type VII$_h$ model is not compatible with measured cosmological parameters, despite the additional freedom from adding dark energy. It is worth reiterating, however, that the serendipitous discovery of a theoretically derived template that correlates well with the data also happens to resolve several anomalies that cannot be explained in the standard picture. These particular models may not be viable, but lacking any plausible scenario for systematics or foregrounds to be the source of the anomalies, non-standard models that reproduce a similar morphology merit continued interest.

ACKNOWLEDGMENTS

We are grateful to S. D. M. White for useful discussions and suggestions. SH was funded by a Killam PostDoctoral Fellowship. We acknowledge use of the HEALPix software (Górski et al. 2005) and analysis package for deriving some results in this paper. We also acknowledge use of the Legacy Archive for Microwave Background Data Analysis (LAMBDA).

REFERENCES

Barrow, J. D., 1976, MNRAS, 175, 359
Barrow, J. D., 1984, MNRAS, 211, 221
Barrow, J. D., Juszkiewicz, R., & Sonoda, D. H. 1985, MNRAS, 213, 917
Bennett, C. L. et al. 2003a, ApJS, 148, 1
Coley, A. & Hervik, S., 2005, CQGrav, 22, 579 [gr-qc/0409100]
de Oliveira-Costa, A., Tegmark, M., Zaldarriaga, M., & Hamilton, A. 2004, Phys. Rev. D, 69, 063516
Dicus, D. A., & Repko, W. W, Phys. Rev. D, 70, 083527
Efstathiou, G., & Bond, J. R., 1999, MNRAS, 304, 75
Eriksen, H. K., Hansen, F. K., Banday, A. J., Górski, K. M., & Lilje, P. B. 2004, ApJ, 605, 14

Freedman, W. L., et al. , 2001, ApJ, 553, 47
Górski, K. M., Hivon, E., Banday, A. J., Wandelt, B. D., Hansen, F. K., Reinecke, M., & Bartelmann, M. 2005, ApJ, 622, 759
Hansen, F. K., Balbi, A.,Banday, A. J., & Górski, K. M. 2004a, MNRAS, 354, 905
Hansen, F. K., Banday, A. J., & Górski, K. M. 2004b, MNRAS, 354, 641
Hervik, S., van den Hoogen, R., & Coley, A., 2005a, CQGrav, 22, 607 [gr-qc/0409106]
Hervik, S., van den Hoogen, R.J., Lim, W.C., & Coley, A.A., 2005b, CQGrav, in press [gr-qc/0509032]
Wainwright, J., & Ellis, G. F. R., eds., 1997, Dynamical Systems in Cosmology (Cambridge University Press)
Jaffe, T. R., Banday, A. J., Eriksen, H. K., Górski, K. M., & Hansen, F. K., 2005, ApJ, 629, L1
Jaffe, T. R., Banday, A. J., Eriksen, H. K., Górski, K. M., & Hansen, F. K., 2005, ApJ, submitted
Juszkiewicz, R., Bajtlik, S., & Górski, K., 1983, MNRAS, 204, 63p
Knop, R. A., et al. , 2003, ApJ, 598, 102
Kolatt, T. S. & Lahav, O., 2001, MNRAS, 323, 859
Land, K., & Maguijo, J., 2005, [astro-ph/0509752]
Lewis, A., & Bridle, S., 2003, PRD, 66, 103511
Matzner, R., Rothman, T., & Ellis, G. F. R., 1986, Phys. Rev. D, 34, 2926
Padmanabhan, T., Phys. Rep., 380, 235
Sanchez, A. G., Baugh, C. M., Percival,W. J., Peacock,J. A., Padilla, N. D., Cole, S., Frenk, C. S., & Norberg, P., 2005, MNRAS, in press, [astro-ph/0507583]
Spergel, D. N., et al. , 2003, ApJS, 148, 175S
Tegmark, M., et al. , 2004, PRD, 69, 103501
Vielva, P., Martínez-González, E., Barreiro, R. B., Sanz, J. L., & Cayón, L. 2004, ApJ, 609, 22
Wang, Y., Kostov, V, Freese, K., Frieman, J. A., Gondolo, P., 2004, JCAP, 12, 3